Supplementary Data

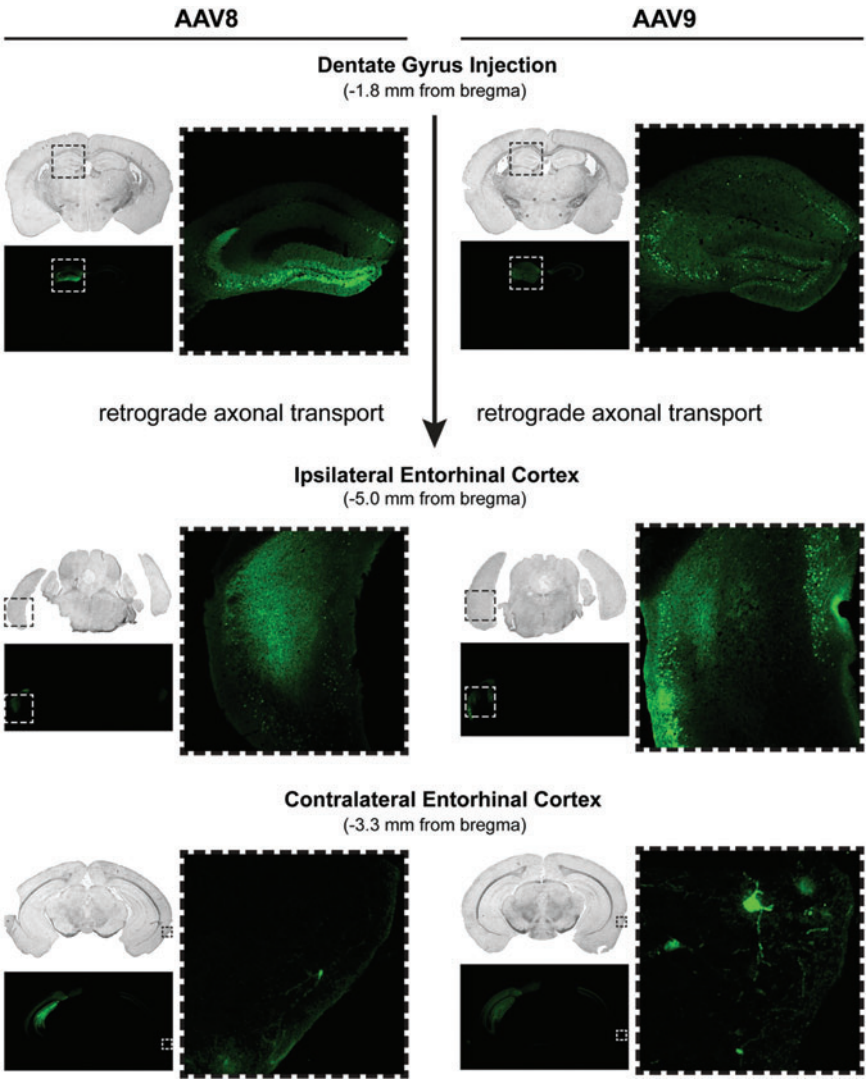

SUPPLEMENTARY FIG. S1. EGFP is expressed at both local and distal sites after dentate gyrus injection of AAV8 and AAV9. Cryosections immediately adjacent to those utilized for ISH (Fig. 6) were immunohistochemically stained for the eGFP transgene product (green). For each brain region, phase contrast and eGFP epifluorescence of the whole cryosection are shown on the left (1.5×objective), alongside eGFP epifluorescence of the region of interest on the right (5×objective). The location of the region of interest is indicated by a box on both 1.5×sections. Cells local to the dentate injection exhibited much stronger fluorescence than cells at distal sites. Thus, the 5×eGFP exposure in the second and third rows was increased from 25 to 300 msec, and the 1.5×eGFP exposure in the second row was increased from 300 msec to 1 sec, in order to visualize distal eGFP. Thresholds of fluorescent images were adjusted to improve visibility; all images within each row were acquired with identical parameters and were adjusted identically. Both serotypes exhibited strong local eGFP expression within DG and CA3, as well as eGFP expression within retrogradely transduced cells of ipsilateral and contralateral EC. Although both serotypes induced widespread transduction of cell bodies in EC, AAV9 appeared to mediate stronger and brighter distal eGFP expression. AAV, adeno-associated virus; ISH *in situ* hybridization.

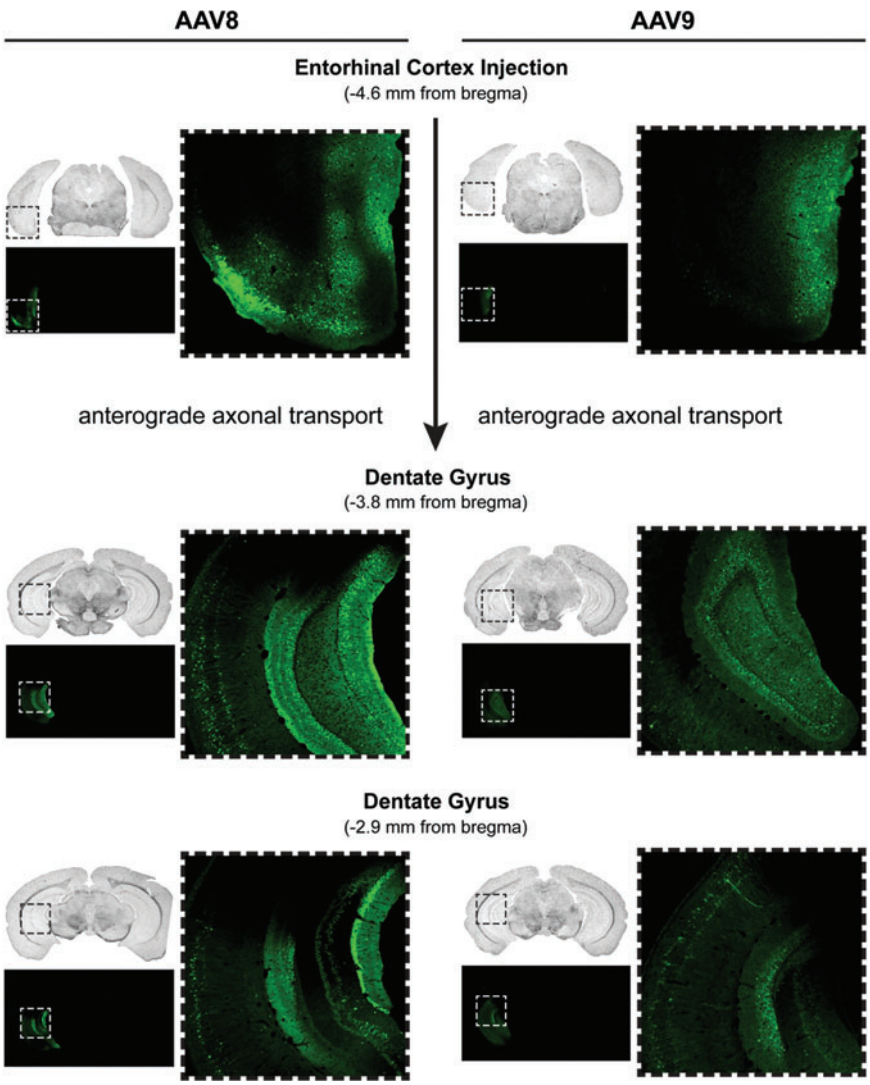

SUPPLEMENTARY FIG. S2. EGFP is expressed at both local and distal sites after entorhinal injection of AAV8 and AAV9. Cryosections immediately adjacent to those utilized for ISH (Fig. 7) were immunohistochemically stained for the eGFP transgene product (green). For each brain region, phase contrast and eGFP epifluorescence of the whole cryosection are shown on the left (1.5×objective), alongside eGFP epifluorescence of the region of interest on the right (5×objective). The location of the region of interest is indicated by a box on both 1.5×sections. Thresholds of fluorescent images were adjusted to improve visibility; all images within each row were acquired with identical parameters and were adjusted identically. Both serotypes induced strong local eGFP expression within EC, although eGFP expression in lateral EC appeared to be more intense with AAV8. EGFP-filled axons from transduced entorhinal projection neurons were brightly fluorescent within the molecular layer of caudal DG. Cell bodies within the granule layer, the projection targets of these entorhinal axons, were observed to strongly express eGFP, indicative of anterograde transport and transduction of second-order cells by both serotypes. EGFP-positive cells were also observed within CA1 and CA3, although overall eGFP fluorescence was less intense in these regions than in DG. DG, dentate gyrus; EC, entorhinal cortex.

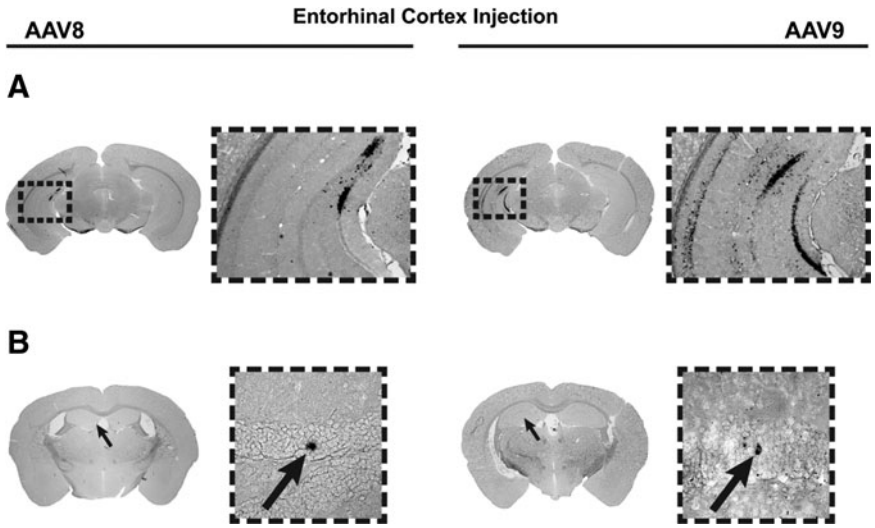

SUPPLEMENTARY FIG. S3. Anterograde transfer of AAV to second-order cells in DG can occur over long distances and with minimal transduction of other hippocampal regions. **(A)** Two mice injected in EC, one with AAV8 (left) and one with AAV9 (right), exhibited widespread ISH staining within DG despite limited transduction of other hippocampal regions. The region of interest was acquired with a 5×objective, and its location is marked with a box on each brain section. The mouse injected with AAV8 (left) exhibited ISH staining exclusively in caudal DG and in EC. The mouse injected with AAV9 (right) exhibited limited staining within the pyrimidal layer of caudal CA1, but staining in caudal DG and in EC was much more intense. These data exclude diffusion from the injection site as a potential route of vector to DG, as hippocampal layers positioned between EC and DG did not contain AAV mRNA. **(B)** Individual cell bodies in rostral DG are ISH-positive after EC injection of AAV8 (left) or AAV9 (right), indicating the presence of AAV mRNA in second-order cells. Within each brain section an arrow indicates the region of interest. Inset images were acquired with a 20×objective and display single ISH-positive cell bodies within the granule layer of DG (arrows). Although transduction of rostral DG was limited in comparison to caudal DG (Fig. 7), isolated ISH-positive cells within rostral DG demonstrate that AAV can undergo anterograde transport over distances of at least 3 mm.